

Driven Polymer Translocation Through a Narrow Pore

David K. Lubensky and David R. Nelson

Department of Physics, Harvard University, Cambridge MA 02138

(October 29, 2021)

Motivated by experiments in which a polynucleotide is driven through a proteinaceous pore by an electric field, we study the diffusive motion of a polymer threaded through a narrow channel with which it may have strong interactions. We show that there is a range of polymer lengths in which the system is approximately translationally invariant, and we develop a coarse-grained description of this regime. From this description, general features of the distribution of times for the polymer to pass through the pore may be deduced. We also introduce a more microscopic model. This model provides a physically reasonable scenario in which, as in experiments, the polymer's speed depends sensitively on its chemical composition, and even on its orientation in the channel. Finally, we point out that the experimental distribution of times for the polymer to pass through the pore is much broader than expected from simple estimates, and speculate on why this might be.

INTRODUCTION

Modern polymer physics has achieved great success with models in which the polymer is regarded as a flexible, uniform “string” whose conformational entropy dominates the system's behavior (de Gennes, 1979; Doi and Edwards, 1986). Although this is usually an excellent description, in some situations other interactions can become important. One example is the insertion of a polymer into a pore of diameter comparable to the size of the chemical repeat units that make up the polymer. Although perhaps unusual with synthetic polymers, such a situation can easily occur in biological systems. For example, Kasianowicz, Brandin, Branton, and Deamer (hereafter KBBD) have recently detected single strands of RNA (polyuridylic acid) passing through a 1.5 nm pore formed by a membrane-bound protein (Kasianowicz et al., 1996). Szabò and coworkers (Szabò et al., 1997; Szabò et al., 1998) and Hanss and coworkers (Hanss et al., 1998) have studied similar systems. In addition to their intrinsic interest, these experiments may eventually lead to a single-molecule RNA and DNA sequencing technique. More generally, most cells must transport macromolecules across membranes in order to function; in several cases, relatively “thick” molecules are believed to pass through nanometer-scale channels. The translocation of polynucleotides through proteic pores has been implicated in a variety of processes, including phage infection and bacterial conjugation (Dreiseikelmann, 1994), the uptake of oligonucleotides by certain organs (Hanss et al., 1998), and transport across the nuclear envelope

in plants (Citovsky and Zambryski, 1993). It has been speculated that some of these transport pathways could eventually prove important in gene therapy (Szabò et al., 1998; Hanss et al., 1998). Similarly, polypeptide-conducting channels play an important role in protein kinesin (Schatz and Dobberstein, 1996; Simon and Blobel, 1991); in a few instances, the translocation may even be driven by electrophoretic effects (Attardi and Schatz, 1988).

There exists a considerable literature on the confinement of polymers in channels of diameter significantly larger than the polymers' persistence length (de Gennes, 1979); well-developed scaling techniques can be used in the theoretical treatment of this regime. Recently, theorists have also shown an interest in the opposite limit of a very narrow, almost point-like hole. For example, several groups have studied the diffusion of polymers across idealized, infinitely thin membranes (Carl, 1998; Di Marzio and Mandell, 1997; Yoon and Deutsch, 1995; Lee and Obukhov, 1996; Park and Sung, 1998a; Park and Sung, 1998b; Sung and Park, 1996). The pore and the membrane are viewed as hard walls whose only interaction with the polymer is steric, and the emphasis is on how the walls' presence decreases the entropy and slows the dynamics of those parts of the polymer outside of the hole. Possible mechanisms for the active transport of polymers through pores in biological systems have also been studied (Peskin et al., 1993; Simon et al., 1992; Sung and Park, 1996).

Inspired largely by the experiments of KBBD, in this paper we consider an different scenario: We study the motion of a homopolymer threaded through a narrow pore with which it has strong interactions. The pore is taken to be sufficiently small that no more than one polymer diameter can fit in it at a given time; in particular, “hairpin” bends are not allowed to pass through the channel. We also put aside the question of how the polymer first enters the hole, focusing instead on the dynamics once one end has been inserted. We then argue that, in the presence of a force driving the polymer through the pore, there should be a regime in which the polymeric degrees of freedom outside of the pore can be neglected, and the system is effectively one-dimensional. In this limiting case we propose a two-tiered picture: a coarse-grained “macroscopic” description of wide validity and a simple “microscopic” model from which the “macroscopic” parameters may be calculated. Our approach follows several authors (Peskin et al., 1993; Simon et al., 1992; Park and Sung, 1998a; Park and Sung, 1998b; Sung and Park, 1996) in viewing the transloca-

tion process as essentially diffusion in one dimension; we differ, however, in emphasizing the role that interactions with the pore itself play in this diffusion process. On the more microscopic level, we include the effects of these interactions through a tilted washboard potential, similar to models of laser mode locking (Haken et al., 1967) or phase dynamics in Josephson junctions (Ambegokar and Halperin, 1969) (see figures 5 and 6). The periodic modulation of the potential reflects the periodicity of the polynucleotide’s sugar-phosphate backbone. The importance of polymer-pore interaction has previously been emphasized by Bezrukov and coworkers (Bezrukov et al., 1996); our model also bears some similarity to work on gel electrophoresis that examines the importance of local “solid friction” forces between the polyelectrolyte and the gel (Deutsch, 1987; Burlatsky and Deutch, 1993; Viovy and Duke, 1994; Burlatsky and Deutch, 1995; Deutsch and Yoon, 1997). Although the macroscopic parameter values for KBBD’s system differ in some respects from those predicted by our microscopic model, we are nonetheless able to make several fairly robust predictions. More importantly, we show how a simple physical mechanism can account for several striking features of the data of KBBD. We thus hope that our work will provide a useful contribution to our understanding of the translocation of polyelectrolytes.

Since our analysis relies heavily on KBBD’s results, the next section sketches some salient features of their data. We then introduce a long length scale “hydrodynamic” description of one-dimensional diffusion and use it to calculate the distribution of passage times for a polymer being driven through a pore. The arguments used to arrive at these results are quite general; in particular, they require few assumptions about the details of the microscopic dynamics of the system. There are, however, circumstances when our approximations break down, and we consider these next. This section also serves to emphasize several aspects of the experiments that will guide our choice of the microscopic model in the succeeding section. After introducing this microscopic model, we use it to calculate a mean drift velocity and an effective diffusion coefficient and compare them to values estimated from KBBD’s data. These comparisons will reveal certain features that cannot be accounted for by our model in its simplest form, so we then discuss possible reasons for the discrepancy, as well as touching briefly on several applications of our calculations. We conclude by summarizing our results and highlighting some issues that remain open.

EXPERIMENTAL BACKGROUND

In the experiments of interest to us, KBBD worked with a *Staphylococcus aureus* α -hemolysin ion channel in an artificial lipid bilayer membrane (diphytanoyl-PC). This channel has the advantage that for many pur-

poses it may be considered always to be open. The α -hemolysin protein has recently been crystallized and an x-ray structure obtained (Song et al., 1996). This reveals a mushroom-shaped complex with a roughly 10 nm long solvent-filled channel. The channel is 1.5 nm in diameter at its narrowest constriction, barely larger than the diameter of a single polynucleotide strand. After inserting a single pore into a bilayer membrane and applying a transmembrane potential of between 110 and 140 mV, KBBD added homopolymeric *single-stranded* DNA or RNA to one side of the membrane, designated *cis*. The samples of polynucleotides had mean lengths on the order of a few hundred nucleotides* and were assumed to be close to monodisperse. After adding the polynucleotides, KBBD monitored the transmembrane ionic current as a function of time. The time series shows a baseline current, modulated by periods on the order of hundreds of microseconds in which the current decreases almost to zero (figure 1, inset). A variety of observations support the interpretation that these blockades were caused by the passage of a polymer through the α -hemolysin channel. The data of KBBD can thus be interpreted as giving measurements of the times required for individual polynucleotides to traverse the membrane under the influence of an electric field.

When these data are displayed as a histogram, with the number of observed events plotted against the length of the blockade (figure 1), one sees that the blockade times fall into three distinct peaks. Of these, the first (“peak 1”) is caused by polymers that enter and retract and thus do not completely cross the membrane, while the other two (“peak 2” and “peak 3”) are both the result of a polymer’s actually passing through the channel. The polymers in peak 3 evidently cross the membrane roughly three times faster than those in peak 2. KBBD made the intriguing suggestion that there are two characteristic times associated with translocation because the polynucleotide can enter the pore in two distinct directions: One peak corresponds to polymers that enter the channel with their 3’ end first, the other to polymers that enter with their 5’ end first. We will show in subsequent sections how such behavior can arise from a simple microscopic model.

A quantity of considerable interest in what follows will be the mean force F driving the polymer through the pore.[†] Clearly F is primarily the result of the electric

*Various groups have measured the persistence length of single-stranded DNA in high salt concentrations to be between 0.75 nm and 1.5 nm (Achter and Felsenfeld, 1971; Smith et al., 1996; Tinland et al., 1997), or roughly 1 to 2 nucleotides, meaning that the polymers used were of order 100 persistence lengths long.

[†]One can define F more precisely as the mean force required to immobilize a given monomer in the pore, where the average is taken over time and over all of the monomers in a given polymer. Thus F does not include hydrodynamic

field acting on the polymer. Since a long, narrow channel has a much larger electrical resistance than the macroscopic volumes of solution on either side of the membrane, any voltage V applied to the system should fall almost entirely across the α -hemolysin pore. The charge on each nucleotide is just the electron charge e , so the electrostatic energy gained by moving one nucleotide through the pore is eV . This suggests that F is roughly

$$F \approx \frac{eV}{a} \approx 5 \frac{k_B T}{a}, \quad (1)$$

where $a \approx 6\text{\AA}$ is the length of a nucleotide, and the second equality holds for $V \approx 125\text{mV}$. For most of the rest of the paper, we will assume that F takes this value, and many of our arguments will be based on the fact that F is thus quite large when expressed in appropriate units. Some effects that could modify F are considered in the discussion section and in appendix C.

Before presenting our model, we would finally like to review the experimental evidence that the interactions between the polymer and the α -hemolysin pore do indeed play the dominant role in KBBD's experiments. We have already mentioned the existence of two distinct characteristic times for the polymer to cross the membrane. Such a result is easiest to interpret if one believes that the polymer's speed is determined by interactions between the polymer and the narrow channel constriction, where molecular scale asymmetries could be important. Similarly, recent data show that homopolynucleotides of different bases can move at strikingly different speeds (Dan Branton, Harvard University, personal communication): poly[U] is of order 20 times faster than poly[dA]. Although chemical differences certainly can lead to variations in polymer properties such as the persistence length, we believe that such strong dependence on molecular details can more easily be explained if we focus on the pore region. Finally, even the fastest polynucleotides pass through the pore far more slowly than simple estimates of hydrodynamic drag would suggest: Model the pore as a cylindrical hole of radius R and the part of the polymer in the pore as a cylinder of radius r . Then, when the polymer moves with speed v , the drag force per length on the part in the pore is roughly $2\pi\eta rv/(R-r)$. Electrophoretic effects change this result very little (see appendix C). For a polynucleotide in an α -hemolysin channel, $r/(R-r)$ is somewhat larger than unity, and the total length of the "cylinder" is roughly 50\AA . According to scaling arguments of Lee and Obukhov (Lee and Obukhov, 1996), the contri-

bution to the drag force from the ends of the polymer outside the channel is only $2 \times 6\pi\eta bv$, where η is the solvent viscosity, and the Kuhn length b is between 15 and 30\AA . Even if hydrodynamic interactions are entirely screened by the motion of counterions (as they are for the electrophoresis of an isolated polymer in solution, with screening length of order the monomer size), the drag on those parts of the polymer in solution cannot be larger than roughly $4\pi\eta Lv$. If one substitutes typical parameter values for KBBD's experiments and balances the sum of these drag forces with the naive driving force of $5k_B T$ per nucleotide, one finds that the polymer would be expected to move through the pore at a rate of roughly 10^8 nucleotides/second, 100 times faster than observed. The three observations of this paragraph, taken together, certainly suggest that we focus on the degrees of freedom in the pore when trying to understand the experiments of KBBD.

COARSE-GRAINED DESCRIPTION

Motivation and Governing Equation

This section, and most of the rest of the paper, is concerned with predicting distributions of blockage times of the sort shown in figure 1. It is now well-established in condensed matter physics that the form of the slow, long length-scale dynamics of a system is often determined by the system's symmetries and conservation laws. All microscopic details are subsumed in phenomenological coupling constants and transport coefficients. In this spirit, we would like to obtain a coarse-grained equation for the probability $P(x,t)$ that a contour length x of the polymer's backbone has passed through the pore at time t . (The variable x is defined so that if the polymer backbone has length L , $x = 0$ when the polymer has just started in the pore and $x = L$ when it has reached the other side). For such a "hydrodynamic" description to make sense, several conditions must be met. One is that the polymer length L be much larger than the distance a between successive nucleotides. We also demand that the dissolved counterions (as well as the solvent and any other solutes) relax quickly compared to the translocating polymer, in order that we may ignore their dynamics. Since the ions are much smaller than a polynucleotide, and consequently diffuse much faster, this condition should not be difficult to satisfy. Finally, our task will be considerably simplified if the microscopic system is (approximately) invariant under translations by an integer multiple of a in either direction. Then, after averaging over variations on the scale of a single nucleotide, we must obtain a translationally invariant equation. We will give this assumption a firmer basis in the next section. Roughly, however, there should be translational invariance when we can neglect the parts of the polymer outside of the channel, and this in turn should be possible when the interactions

drag forces, nor forces that vanish when averaged over all the monomers. Equivalently, F can be defined by requiring that $\exp(Fa/k_B T)$ be the ratio of the probabilities that the polymer will move forward one base to the probability that it will move backwards one base, again appropriately averaged over all monomers.

between the polymer and the pore are strong enough.

Under the conditions just outlined, the (probability) density of the polymer is the only conserved variable, and it is relatively straight-forward to write down the coarse-grained hydrodynamic equation for P . Because there is only a single polymer (or, equivalently, a “gas” of non-interacting polymers going through the same hole), the probability current j , defined by $\partial P/\partial t + \partial j/\partial x = 0$ must be linear in P . The lowest order allowed terms are then proportional to P and to $\partial P/\partial x$:

$$j(x, t) = vP(x, t) - D \frac{\partial P(x, t)}{\partial x}. \quad (2)$$

The first term is permitted because there is an electric field driving the system. P then satisfies the familiar equation for diffusion with drift,

$$\frac{\partial P}{\partial t} = D \frac{\partial^2 P}{\partial x^2} - v \frac{\partial P}{\partial x}. \quad (3)$$

Here v and D are respectively an average drift velocity and an effective diffusion coefficient. Their values are determined by more microscopic physics; in particular, they may depend nonlinearly on the applied electric field. Eq. 3 may alternatively be derived from a microscopic master equation that is invariant under translations by a . The coefficients v and D are then related to the lowest-lying eigenvalues of the master equation. This connection will be illustrated in a subsequent section.

On the macroscopic level of Eq. 3, all information on the competition between driving and diffusive spreading is encoded in a parameter that we call the diffusive length $l_d \equiv D/v$. Roughly speaking, on length scales less than l_d , the polymer’s motion is little affected by the presence of the bias from the electric field, while on scales larger than l_d , the driving dominates. Indeed, if Eq. 3 described a rigid particle diffusing in one dimension under the influence of a uniform force f , an Einstein relation would hold, and we would have $v = Df/(k_B T)$, and $l_d = k_B T/f$. Thus, in this case, l_d is precisely the length over which the driving force does a quantity $k_B T$ of work. In the remainder of this section, we will often assume that the length L of the polymer is larger than l_d , a condition satisfied by KBBB’s data.

Distribution of Passage Times

We now propose to calculate a distribution of passage times of the sort measured by KBBB. This section will show that, for given v and D , the probability $\psi(t)$ that the polynucleotide takes a time t to pass through the channel has only one peak. Thus, the presence of two peaks in KBBB’s data must be explained by the assumption that different physical situations give rise to different values of v and D . Subsequent sections will argue that a polynucleotide passing through the pore with its 3’ end

first can indeed have an average velocity that is significantly different from one passing through with its 5’ end first. This section, however, is confined to the calculation of the passage times for fixed parameter values. The distribution $\psi(t)$ we obtain should thus be compared to a single peak in the data of KBBB.

One can easily estimate the first few cumulants of this distribution. If a polymer of length L moves with average velocity v , one expects that the mean time to pass through the channel should be $\langle t \rangle \approx L/v$. Likewise, the variance in the distance traveled in a time $\langle t \rangle$ is $(\Delta x)^2 = 2D\langle t \rangle$. It would then seem reasonable that the variance in arrival times should be $\Delta t^2 \equiv \langle (t - \langle t \rangle)^2 \rangle \approx (\Delta x)^2/v^2$, or $\Delta t^2 \approx 2DL/v^3$. These conclusions are in fact roughly correct for a sufficiently long polymer. One might expect corrections, however, because some fraction of the polymers that enter the pore will leave again from the same side instead of passing all the way through. On average, these will be the “slower” molecules: Those that spend a significant time with only the tip of the polymer inserted in the channel are far more likely to fall back out than are those that are quickly driven through the hole. Thus, only “faster” chains tend to enter into the calculation of the mean transit time, decreasing $\langle t \rangle$. This effect is most pronounced for small L/l_d , because only molecules within l_d of the *cis* side have an appreciable chance of “backing out” instead of exiting on the *trans* side. Indeed, when $L \ll l_d$, the driving should be negligible, and we expect $\langle t \rangle$ to approach its $v = 0$ value $L^2/6D$. To determine the precise form of this crossover, we must turn to a more detailed calculation.

This calculation can be formulated as one of a well-studied class of problems known as first-passage problems (Risken, 1984; van Kampen, 1992). Essentially, all that is required is to solve Eq. 3 on the interval $[0, L]$ with absorbing boundary conditions $P(0) = P(L) = 0$. Then, the current density $j(L)$ at L gives the probability per time that the polymer will leave the pore from the far (*trans*) side, while $-j(0)$ is the probability per time that it will exit from the *cis* side from which it entered. One must also specify the starting point $x_0 \in [0, L]$ of the polymer; in what follows, we always take the limit $x_0 \rightarrow 0$, in keeping with the fact that the polymer starts entirely on the *cis* side of the membrane. The algebraic details of the solution are summarized in appendix A; here we include only a discussion of the main results.

Although exact expressions for $\langle t \rangle$ and Δt may be obtained, it turns out to be more instructive to consider the distribution $\psi(t)$ itself. For arbitrary L/l_d , this can only be expressed as an infinite series, but if terms that become exponentially small as $L^2/(vtl_d) \rightarrow \infty$ are neglected, a comparatively simple analytic expression is obtained:

$$\psi(t) \simeq \frac{v}{2} \sqrt{\frac{l_d}{\pi}} \left(\frac{L^2}{l_d(vt)^{5/2}} - \frac{2}{(vt)^{3/2}} \right) e^{-(vt-L)^2/(4vtl_d)}. \quad (4)$$

Note that this expression is not valid for sufficiently large t , and in particular not for t so large that it predicts that $\psi(t)$ becomes negative. Nonetheless, for values of t near the maximum in $\psi(t)$, i.e. those such that $vt/L \sim \mathcal{O}(1)$, it is accurate to within a percent for L/l_d as small as 4, and correctly reflects the qualitative features of $\psi(t)$ for significantly smaller L/l_d . Figure 2 plots $\psi(t)$ for $L/l_d = 5$; a Gaussian with the same mean and variance is included for comparison. Evidently, $\psi(t)$ is quite skewed, and its mean and maximum are correspondingly well-separated. Thus, $\langle t \rangle$ and Δt are not the best parameters for describing experimental data. Indeed, both cumulants are sensitive to how $\psi(t)$ decays for large t , making them very hard to extract accurately from realistic data sets. A more useful choice of parameters to characterize $\psi(t)$ are the position t_{\max} of its maximum (which satisfies $d\psi/dt|_{t_{\max}} = 0$) and the width δt of the peak. The latter is defined as $\delta t \equiv (t_R - t_L)/2$, where t_R and t_L satisfy $\psi(t_R, t_L) = e^{-1/2}\psi(t_{\max})$; we have chosen a factor of $e^{-1/2}$ instead of the more conventional $1/2$ to facilitate comparison with fits of data to a Gaussian. One expects that as $L/l_d \rightarrow \infty$, t_{\max} and δt should approach $\langle t \rangle$ and Δt , respectively. For example, for large L/l_d we have,

$$t_{\max} = \frac{L}{v} \left(1 - 5\frac{l_d}{L} + \frac{17}{2}\frac{l_d^2}{L^2} + 32\frac{l_d^3}{L^3} + \dots \right). \quad (5)$$

The rapidly growing coefficients indicate that although t_{\max} approaches L/v as L approaches infinity, it falls away from its asymptotic form quite rapidly for finite L .

More generally, one can easily find t_{\max} and δt by numerically solving the equations that define them. Figure 3 plots $\delta t/t_{\max}$ versus the polymer length L . This ratio is especially interesting because it depends only on L/l_d , and not on v and D separately; one can thus use it quickly to estimate L/l_d . In KBBD's data, $\delta t/t_{\max}$ is usually of order 0.5 for a ~ 200 nucleotide chain, suggesting that $L/l_d \approx 5$, or that l_d is of order 40 nucleotides. As figure 4 indicates, in this range t_{\max} already deviates significantly from the naive guess $t_{\max} \approx L/v$. In particular, t_{\max}/L varies by a factor of 2 as L/l_d increases from 5 to 25. With sufficiently good data, this deviation from a strict proportionality to L might well be observable, providing strong confirmation of our quasi one-dimensional picture.

REGIME OF VALIDITY

In the previous section, we argued that a requirement for the validity of a one-dimensional diffusion model was that the system be (approximately) unchanged if the polymer moves an integer number of monomers forwards or backwards in the pore. This section discusses when this condition is satisfied. We begin by dividing the polymer into three parts: the roughly ten nucleotide long

piece that is actually *inside* the channel, and the two "ends", comprising the majority of the nucleotides, *outside* the channel. The pore always contains the same number of bases, so, for the homopolymers, this part of the polymer always satisfies the requirement of translational symmetry. The length of each end "dangling" outside the pore, in contrast, changes with the translocation parameter x , destroying translational invariance. In what follows, we shall argue that under certain conditions this variation may be neglected. Our arguments assume that the parts of the polynucleotide outside the pore may be described by the theories usually applied to long, flexible polymers (de Gennes, 1979; Doi and Edwards, 1986); we thus ignore, for example, hydrogen-bonding and other specific interactions (Cantor and Schimmel, 1980). We also assume that the ion channel is sufficiently long and narrow that any voltage drop falls almost entirely across the channel (see appendix C). The electric field and the solvent flow velocity outside of the channel can then be ignored.

There are two criteria for ignoring the ends of the polymer outside of the pore. First, they should have a characteristic relaxation time that is much faster than the characteristic time for the motion of a monomer through the channel. In the absence of interactions between the polymer and the pore, one would expect diffusion on the scale of a few monomers to be much faster than the relaxation of a long polymer coil, and this inequality could never be satisfied. However, since the nucleotides in the pore can be expected to interact strongly with the confining protein, the requirement is not implausible. The longest time scale of an isolated polymer in solution is the Zimm time $t_Z \approx 0.4\eta R_G^3/(k_B T) \approx 0.4\eta N^{3\nu} b^3/(k_B T)$, where ν is the Flory exponent,[‡] b is the Kuhn segment length (equal to twice the persistence length), η is the solvent viscosity, and $N = L/b$. Substituting in numerical values for a single-stranded polynucleotide in water, one finds that $t_Z \approx N^{3\nu} (3.2 \times 10^{-4} \mu\text{sec})$. If we imagine that the polymer moves a monomer through the channel by hopping over an energetic barrier (an idea to be considered in more detail when we introduce our microscopic model), then in the limit of strong driving, the translocation speed is simply $v = a/t_{\text{pore}}$, where t_{pore} is the longest relaxation time of the part of the polymer in the pore. Substituting numerical values for poly[U], we find $t_{\text{pore}} = a/v \approx 1.5 \mu\text{sec}$. Comparing this figure to t_Z , we see that the two become of the same order when N is of order 150, corresponding to a length of polymer of roughly 300 nucleotides protruding from each side of the pore. Of course, for polymers that traverse the mem-

[‡]In principle, $\nu \approx 0.6$ for a long polymer in a good solvent. However, even with the longest available chains, ν is never observed experimentally to be larger than 0.55 (Doi and Edwards, 1986), so we use this value for specific numerical calculations.

brane more slowly, as is the case for poly[dA], the value of N above $t_Z \gtrsim t_{\text{pore}}$ can be significantly larger.

As long as the dynamics of the polymer outside of the pore are fast compared to the dynamics in the pore, one need not treat the external degrees of freedom explicitly. Instead, they affect the motion of the polymer only through a contribution $\mathcal{F}(x)$ to its free energy and through the increased drag they contribute.[§] Lee and Obukhov's scaling argument (Lee and Obukhov, 1996) implies that their effect on the drag is independent of the length of polymer on a given side of the membrane. On the other hand, in order for us to be able to neglect \mathcal{F} , $d\mathcal{F}/dx$ must be small compared to the force F driving translocation. Denote the free energy of the coil on the *cis* side of the membrane by $\mathcal{F}_C(x)$ and that of the coil on the *trans* side by $\mathcal{F}_T(x)$; their sum is $\mathcal{F}(x)$. Sung and Park pointed out that \mathcal{F}_C and \mathcal{F}_T are simply the free energies of a polymer grafted by one end to a planar surface (Sung and Park, 1996). For a polymer of length x , this entropic free energy is known to be proportional to $k_B T \ln(x/b)$, with a coefficient of order unity that depends on whether excluded volume effects are important (Binder, 1983). Ignoring the few monomers actually in the channel, the lengths of polymer on the *cis* and *trans* sides of the barrier are x and $L - x$, respectively, so

$$\mathcal{F}(x) \propto k_B T \left[\ln\left(\frac{x}{b}\right) + \ln\left(\frac{L-x}{b}\right) \right]. \quad (6)$$

For a chain that is a fixed fraction of the way through the hole (i.e. for fixed x/L), $d\mathcal{F}/dx$ vanishes like $1/L$. Further, it makes little sense to consider $x < a$, where a is the length of a single monomer, so we must always have $d\mathcal{F}/dx \lesssim k_B T/a$. Typical values will be much smaller than this bound. The driving force $F \approx 5k_B T/a$ thus greatly exceeds $d\mathcal{F}/dx$; indeed, since the polymers used by KBBD are several hundred nucleotides long, F is more than a factor of 100 larger than a typical value of $d\mathcal{F}/dx$. In sum, we have shown that in the window of polymer lengths

$$\frac{k_B T}{F a} \ll N \ll \left(\frac{k_B T a}{\eta b^3 v}\right)^{1/3\nu} \quad (7)$$

the polymer is short enough to relax quickly, but long enough that the entropic barrier to crossing the membrane is not too steep. For lengths in this window, the ends of the chain hanging outside of the pore can be neglected compared to the monomers inside the pore. Since the system studied by KBBD falls within this window,

[§]Here, we assume that v is sufficiently small that the parts of the polymer outside the pore are essentially in equilibrium. On purely dimensional grounds, this must be true when $t_Z \ll N^y (b/v)$ for some non-negative exponent y , a requirement that is met in KBBD's experiments.

we are justified in using simple one-dimensional models to describe it.

MICROSCOPIC MODEL OF THE PORE

Until now, we have avoided specifying the physics of the interactions within the pore. In this section, we present a simple phenomenological model of these interactions. Our main goal is to understand physically how the parameters v and D can vary sufficiently to explain experimental facts like the difference in velocities between polymers moving forwards and backwards.

Description of the Model

We begin by focusing on the polymer backbone, whose coordinate x tells us what fraction of the polymer chain has passed through the channel. If the motion of the backbone is sufficiently slow compared to all the other degrees of freedom in the pore, then we can take x to be the only dynamical variable in the problem. The remaining degrees of freedom are then described by a free energy $\Phi(x)$ that depends on the polymer translocation parameter x . The potential $\Phi(x)$ can, for example, be expected to have contributions from electrostatic interactions between the polymer and the α -hemolysin heptamer. Two unit charges separated by 1 Å in water have an energy of about $6k_B T$ at room temperature; since both polynucleotide and protein have completely ionized groups in physiological pH, it is thus plausible that typical values of Φ should be at least on the order of several $k_B T$. We split Φ into a mean slope F determined by the applied voltage drop and a part $U(x)$ that captures the details of the polymer's interactions with the pore: $\Phi(x) = U(x) - Fx$.** For homopolymers (provided we continue to neglect the degrees of freedom outside the pore), $U(x)$ is periodic, with period $a = 1$ nucleotide. F is precisely the mean force introduced in Eq. 1, and is equal to eV/a in the simplest picture.

Our problem is now formally no different from that of a point particle diffusing in a periodic potential U and driven by a constant force F . The probability $P(x)$ of finding such a particle at a point x is governed by a Smoluchowski equation,

$$\begin{aligned} \frac{\partial P}{\partial t} &= D_0 \frac{\partial}{\partial x} \left[\frac{\partial P}{\partial x} + \frac{U'(x) - F}{k_B T} P \right] \\ &\equiv \mathcal{L}P. \end{aligned} \quad (8)$$

**In principle, U could depend on the applied voltage (and hence on F). We ignore this effect; many of our conclusions will in any case turn out to be insensitive to it.

The “bare” diffusion constant D_0 is related through an Einstein relation to some suitable drag force on the polymer in the channel. It is not to be confused with the “effective” diffusion constant D that includes the effects of U and describes the polymer’s motion on length scales much larger than a .

It is helpful both for numerical work and for intuition building to have a concrete idea of the simplest form $U(x)$ could take. In particular, such a simplified “cartoon” will give us an idea of the minimum number of parameters needed to describe the gross features of the potential. A natural choice for such a $U(x)$ is a sawtooth potential of the sort sketched in figure 5. It is described by two dimensionless parameters, the peak height $U_0/k_B T$ and the asymmetry parameter α . When $\alpha = 1/2$, the potential is perfectly symmetrical, while $\alpha = 0$ or 1 corresponds to maximal asymmetry. In addition to $U(x)$, the full potential Φ contains a term proportional to the driving force F , which figures in the dimensionless group $Fa/k_B T$. Thus, to specify our potential fully, we require the three dimensionless parameters $U_0/k_B T$, α , and $Fa/k_B T$, as well as D_0 and the repeat distance a , which set a time and a length scale. More generally, we expect that any form of $U(x)$ with only one peak per period will be roughly characterized by a peak height U_0 (equal to the difference between the minimum and the maximum values of $U(x)$), and an asymmetry α (defined as the distance between a minimum in $U(x)$ and the next maximum to the right, divided by a). While we have no *a priori* information about α , we have suggested that U_0 should be of order several $k_B T$, and have argued $Fa/k_B T \approx 5$ for KBBB’s experiments.

Because the time required to diffuse over a barrier depends exponentially on the barrier height, small differences in U_0 can lead to significant changes in translocation speed, consistent with KBBB’s observations. Further, if $U(x)$ is asymmetrical, forces F and $-F$ will lead to different barrier heights, and thus to different mean drift speeds for the diffusing polymer. Figure 6 illustrates this point. It thus appears plausible that a polymer moving through the pore with its 5’ end first could travel at a very different speed from one going through the pore 3’ end first. There is, however, one additional complication. As shown in figure 7, three different “vector” quantities can be oriented relative to the membrane: the applied electric field, the α -hemolysin pore, and the DNA. Each can point towards the *cis* or the *trans* chamber. With, say, the pore orientation held fixed, there are thus four possible situations. The two that have been realized in the experiments of KBBB are related by a flip of the polymer, while transforming $F \mapsto -F$ (or equivalently $U(x) \mapsto U(-x)$) in our model amounts to changing the direction of the field. Thus, although a velocity difference of a factor of 3 can clearly be accounted for by reasonable choices of parameters, we cannot quantitatively address how the two peaks in KBBB’s experiments are related. Once all four possible situations have been explored experimentally, however, it should be possible, for example,

to estimate the value of α by comparing data for the appropriate pairs of situations.

Effective Mobility and Diffusion Coefficient

We now turn to the task of calculating the parameters v and D that describe the behavior of Eq. 8 on long length scales. Several approaches are available; in this section, we will describe the results of an analysis based on ideas of Risken (Risen, 1984). Details of the calculation, which relies on an eigenfunction expansion, are given in appendix B. In the most general case, v and D have fairly complicated forms, but relatively simple limiting cases capture most of the relevant behavior. For example, one finds (le Doussal and Vinokur, 1995; Scheidl, 1995)

$$\frac{1}{v} = \frac{1}{D_0} \int_0^\infty dz e^{-Fz/k_B T} \int_0^a \frac{dx}{a} e^{[U(x+z)-U(x)]/k_B T}, \quad (9)$$

from which a number of limiting behaviors can be extracted. Several equivalent expressions for v , as well as a similar, but more involved, expression for D , can also be obtained.

Figure 8 plots the velocity v versus F for polymers traveling in two different directions in the same (asymmetric) potential. At typical values of F , differences in velocity between forwards and backwards motion of a factor of 3 or more are easily obtained. Likewise, the calculated velocities are much slower than they would have been in the absence of a potential.

One can gain more quantitative insight into both of these observations by studying how v and D behave in various limiting cases. Relegating the derivations to appendix B, we next consider several such expressions. Three cases are particularly of interest: large and small driving force F , and large potential barriers U_0 (the case of small U_0 corresponds to the absence of a potential and was discussed earlier). For small F , v and D must satisfy an Einstein relation. Indeed, in this limit one finds,

$$v = \frac{D_0 F}{k_B T} \frac{1}{I_1^{(0)} I_2^{(0)}} \left[1 + \mathcal{O}\left(\frac{Fa}{k_B T}\right) \right]$$

$$D = D_0 \frac{1}{I_1^{(0)} I_2^{(0)}} \left[1 + \mathcal{O}\left(\frac{Fa}{k_B T}\right) \right], \quad (10)$$

where

$$I_1^{(0)} = \int_0^a \frac{dx}{a} e^{U(x)/k_B T}$$

$$I_2^{(0)} = \int_0^a \frac{dx}{a} e^{-U(x)/k_B T}. \quad (11)$$

Thus, $v/D = F/k_B T$, as the fluctuation-dissipation theorem requires, but the effective diffusion coefficient D is reduced from its bare value D_0 by a factor that grows

exponentially with the characteristic height of the potential. Perhaps more surprising is the fact that a linear-response-like regime is also reached for sufficiently large F . As $F \rightarrow \infty$,

$$\begin{aligned} v &= D_0 F \left[1 + \mathcal{O}\left(\frac{U_0}{Fa}\right)^2 \right] \\ D &= D_0 \left[1 + \mathcal{O}\left(\frac{U_0}{Fa}\right)^2 \right]. \end{aligned} \quad (12)$$

The physical content of this result is that when F is much larger than a typical force derived from $U(x)$, $\Phi'(x) \approx -F$, and contributions from U may be neglected entirely. In the opposite limit of large U_0 , one might expect that the diffusion process can essentially be described as hopping from one potential minimum to the next. Approximate formulas based on the Kramers escape rate (van Kampen, 1992) should then apply. In fact, for large U_0 one finds

$$v \simeq \frac{D_0}{aI_1^{(0)}I_2^{(0)}} \left[e^{\alpha Fa/k_B T} - e^{-(1-\alpha)Fa/k_B T} \right] \quad (13)$$

and

$$D \simeq \frac{D_0}{2I_1^{(0)}I_2^{(0)}} \left[e^{\alpha Fa/k_B T} + e^{-(1-\alpha)Fa/k_B T} \right]. \quad (14)$$

As before, we select the origin of $U(x)$ so that its maximum and minimum in each period occur at points $x_{\max} > x_{\min}$, with $x_{\max} - x_{\min} = \alpha a$.

We have already estimated from KBBB's data that $l_d \equiv D/v \approx 40a$. A striking feature of the asymptotic forms Eq. 10 through Eq. 14 just obtained is that all three imply a much smaller value. As we noted when we introduced the parameter l_d , the linear response results both yield $l_d = k_B T/F$; given our naive estimate $Fa/k_B T \approx 5$, we find $l_d \approx a/5 \ll 40a$. For U_0 large enough that the "hopping" approximation of Eq. 14 applies, this order of magnitude is little changed even as $F \rightarrow \infty$. Indeed, in this limit Eq. 14 gives $l_d = a/2$. It is of course possible that some particular form of $U(x)$ with finite U_0 and F might lead to a value of l_d of order $40a$. It seems more likely, however, that l_d interpolates reasonably smoothly among its various limiting values. The inset to figure 8 illustrates this point for the sawtooth potential introduced earlier. Although v and D each separately can depend strongly on the shape of $U(x)$, their ratio is far less sensitive. We are thus led to one of the central conclusions of this paper: While many aspects of KBBB's results can be qualitatively explained by a model of diffusion in a one-dimensional periodic potential, the observed width of their peaks is inconsistent with this model if one takes $Fa \approx 5k_B T$.

DISCUSSION

In the previous section, we argued that the peaks in KBBB's distribution of first passage times are

much wider than is consistent with our minimal one-dimensional model. It is not difficult to suggest reasons why this might be the case. Perhaps the most obvious is that $Fa/k_B T$ could differ significantly from 5. Not only would a decrease of a factor of 100 in F bring our prediction for l_d into line with experimental observations, it would also explain the polymer's unexpectedly slow translocation speed. At least two effects might decrease F . First, unless the pore has infinite resistance, not all of the applied voltage drop V will be across the pore. Although the large ($\sim \text{M}\Omega$) resistance of the α -hemolysin channel makes it unlikely that this mechanism could diminish F by orders of magnitude, it certainly leads to some decrease. Second, the fact that there is a nonzero ionic current flowing through the pore while the polymer is translocating means that the motion of the polymer itself need not satisfy detailed balance. That is, the *error rate*, or ratio of the probabilities of moving forward one base to moving backwards one base, is no longer required to be equal to $\exp(eV/k_B T)$. To use a somewhat different language, as the counterions are forced through the pore by the electric field, they entrain some of the solvent along with them. This solvent flow exerts an additional drag force on the polymer, and this drag contributes to the mean force F . As a result, the electrophoretic mobility of the polymer in the channel is not in general equal to its hydrodynamic mobility multiplied by its charge. Appendix C presents simple estimates based on continuum mechanics that suggest that both of these effects are small. These estimates, however, make a number of simplifications; indeed, even the validity of the continuum equations is not assured on the nanometer scale. Given the importance of a large value of $Fa/k_B T$ to any attempts to sequence polynucleotides using the α -hemolysin pore, it thus seems desirable to verify experimentally that it is indeed approximately 5.

Although a smaller than expected driving force is certainly one mechanism that would generate wider peaks, others exist that do not require a large error rate. In many ways, our most poorly justified assumption is that the motion of the polymer backbone through the pore is much slower than the relaxation of every other degree of freedom in the system, so we begin by considering what might happen if this assumption were to break down. For example, the protonation state of the open α -hemolysin channel is known to fluctuate on a much slower time scale than the characteristic polymer time $a/v \sim 1\mu\text{sec}$ (Kasianowicz et al., 1995), and the energy barrier to moving a base through the pore might change significantly when the protonation state changes. It is instructive to consider a naive extension of our one-dimensional model meant crudely to describe such a situation. Suppose that the pore + polymer system can be in one of two states, state 1, in which the polymer backbone can diffuse freely, and state 2, in which the backbone is trapped and cannot move. Let there be a transition rate (per time) ω_{ij} from state i to state j . This situation bears some similarities to popular mod-

els of motor proteins (Jülicher et al., 1997), but with the important difference that the ratio ω_{12}/ω_{21} need not violate detailed balance; a similar description has also recently been proposed for the one-dimensional motion of RNA polymerase along a polynucleotide (Jülicher and Bruinsma, 1998). If $P_i(x)$ is the probability that the system is in state i and that a length x of polymer has passed through the pore, the long time diffusion of the system is governed by equations of the form

$$\frac{\partial P_1}{\partial t} = D_1 \frac{\partial^2 P_1}{\partial x^2} - v_1 \frac{\partial P_1}{\partial x} - \omega_{12} P_1 + \omega_{21} P_2 \quad (15)$$

$$\frac{\partial P_2}{\partial t} = \omega_{12} P_1 - \omega_{21} P_2. \quad (16)$$

In state 2, the motion is arrested, so both the velocity and the diffusion coefficient vanish. Just as in the one-dimensional, periodic case (appendix B), this model leads to a spreading Gaussian wave packet, with velocity and diffusion coefficient determined by the behavior of the eigenvalues near zero. One finds a velocity

$$v = \frac{v_1}{2} \left(1 + \frac{\Delta\omega}{\omega} \right), \quad (17)$$

and a diffusion coefficient

$$D = \frac{D_1}{2} \left(1 + \frac{\Delta\omega}{\omega} \right) + \frac{v_1^2}{2\omega} \left(1 - \frac{(\Delta\omega)^2}{\omega^2} \right), \quad (18)$$

where $\Delta\omega = \omega_{21} - \omega_{12}$ and $\omega = \omega_{12} + \omega_{21}$. Thus, if $v_1 \neq 0$ and ω and $\Delta\omega$ are chosen properly, $l_d = D/v$ can be made arbitrarily large. This is true even if D_1/v_1 remains of order a . Thus, even in this simple example, broad peaks are possible as soon as one relaxes the constraint that the model only contain one degree of freedom.

In addition to the possibility that there is more than one slow degree of freedom, many other factors could contribute to the wide blockage time distributions observed by KBBB. For example, the observed peaks could reflect not the distribution in passage times for polymers of a given length, but the length distribution of the polymers themselves. Although the polydispersity of the poly[U] samples used by KBBB was not well characterized, no qualitative differences were seen with a perfectly monodisperse sample of DNA (Dan Branton, Harvard University, personal communication), suggesting that polydispersity is not the culprit. Similarly, we calculated the free energy \mathcal{F} of the parts of the polynucleotide outside the pore using a model that applies to conventional polymers above the theta point. If \mathcal{F} took a different form, we might not be able to neglect it. In particular, significant asymmetries between the two sides of the membrane could result in a non-electrical contribution to the driving force (Park and Sung, 1998b; Di Marzio and Mandell, 1997; Carl, 1998). For example, if the polynucleotide adsorbs weakly on one side of the membrane, there would be a force towards the adsorbing side of order $f k_B T/a$, where f is the fraction of adsorbed

monomers. A similar effect could be obtained by confining the polymer on only one side of the membrane. Indeed, for sequencing applications, it might be useful intentionally to introduce an asymmetry as a way to manipulate the polymer's speed and error rate without affecting the ionic current. Similarly, the current can in principle be varied with little effect on the polymer by putting a high concentration of macroions (e.g. colloidal particles) on one side of the membrane. This would induce a concentration gradient in their counterions that tended to drive the ions across the membrane.

Finally, we would like to touch on one other issue of particular relevance to efforts to sequence polynucleotides as they pass through the pore. All of our results up to this point have been strictly valid only for homopolymers. Since it is known that diffusion in random media can be qualitatively different from diffusion in ordered systems (Bouchaud and Georges, 1990), it is worth asking whether we expect any important changes when the homopolymer is replaced by a random heteropolymer. As long as the assumptions leading to our model of diffusion in a one-dimensional, periodic medium hold, one can argue that the effect of using heteropolymeric DNA would be to modify the potential $U(x)$. Rather than having an identical form within each unit cell of length a , $U(x)$ might take one of four different shapes, corresponding to four different bases. It is known that one-dimensional diffusion becomes anomalous when $\overline{[U(x) - U(0)]^2} \rightarrow \infty$ as $x \rightarrow \infty$, where the overbar indicates an average with respect to the random distribution of bases (Bouchaud and Georges, 1990; le Doussal and Vinokur, 1995; Scheidl, 1995). In biological DNA sequences, it is believed that successive bases are either uncorrelated or have correlations that decay algebraically with distance (Herzel et al., 1998; Stanley et al., 1992). In either case, $\overline{[U(x) - U(0)]^2}$ remains bounded for large x . Thus, within the simple one-dimensional model, no qualitatively new behavior would result from replacing homopolymers with heteropolymers. This is what one would expect to observe for short polynucleotides like those used by KBBB. It is worth mentioning, however, that this conclusion is sensitive to other effects. For example, the electrophoretic mobility of the polymer in the pore presumably has some sequence dependence; this would lead to an effective short-range correlated random force on the polymer. Such a random force, however small, would in principle result in anomalous diffusion on sufficiently long length scales (Bouchaud and Georges, 1990; Fisher et al., 1998).

CONCLUSION

The central idea of this paper was first presented in the introduction: In the experiments of KBBB, and likely in other examples of the translocation of biopolymers, the channel through which the polymer passes cannot be viewed simply as a set of hard, homogeneous walls.

Rather, more specific interactions between the polymer and the channel must be taken into account. Indeed, we have argued that there is a regime in which polymer-pore interactions dominate, allowing a quasi-one-dimensional description of the translocation process. One immediate consequence of this observation is that on long enough length scales, the transport of the polymer through the pore is governed by a simple phenomenological equation. Starting from this equation, we have derived several predictions about the polymer's distribution of passage times. For example, we have shown that the polymer's mean translocation time depends linearly on its length only for an extremely long polymer. It is perhaps worth reemphasizing that none of these results depend on any particular microscopic model of the pore. In contrast, several important qualitative observations of KBBB can be understood in terms of a more microscopic picture involving a "tilted washboard" potential. The tilted washboard model also lead us to point out that the distribution of passage times in KBBB's experiments was far broader than one might expect from simple estimates, or indeed from any model with only one degree of freedom. We have suggested several ways that this discrepancy might arise. Some, such as a serious mis-estimate of the mean force F on the polymer, imply an error rate in DNA sequencing of almost 50%. Several others, however, do not require revision of the estimated error rate. Most notable among these are polydispersity in the polymer lengths and a strong coupling between the polymer and another degree of freedom in the pore with slow dynamics. Determining which mechanism is at work in the experiments of KBBB remains an important experimental and theoretical challenge.

Our conclusions suggest several experimental avenues that might be explored in KBBB's or some analogous system. Most obvious would be to try to measure the error rate (or equivalently, the driving force F). At least a rough estimate of $Fa/k_B T$ might be obtained in several ways. Obviously, any experiment in which it is possible to detect the passage of a particular nucleotide through the pore gives one direct access to the error rate. Alternatively, at small enough applied voltage V , it should be possible to observe a linear response regime. Deviations from linear behavior would then be observed at a value of V such that $Fa/k_B T \sim \mathcal{O}(1)$. With linear response data from all four possible relative orientations, it should also be possible to observe that dv/dV is the same for pairs of peaks. More ambitiously, if one could exert a non-electrical force on the polymer strong enough that its mean velocity through the pore fell to zero, this would give a direct measurement of F . Such an experiment might be accomplished with modern micromanipulation techniques.

Other experiments of interest might test the existence of a quasi-one-dimensional regime. With enough data on the length dependence of t_{\max} , for example, it should be possible to observe the predicted deviation from the simple guess $t_{\max} \propto L$. Further, if this data could be

extended to sufficiently long polymers, deviations from the curve of figure 4 would provide information on the crossover to a regime in which the dynamics of the polymer outside the pore are slower than those inside the pore. Once the basic theory has been verified, a number of different directions remain open. For example, a study of the fluctuations of the ionic current with a polymer in the pore could provide evidence about whether there are important slow degrees of freedom other than the polymer backbone itself. Adding a time varying component to the applied voltage in the experiments of KBBB might provide advantages in sequencing applications; the characteristic frequency for motion from one base to the next appears to be a relatively low 10^6 Hertz. The behavior of polymers in very narrow channels is a rich subject that has only begun to be investigated.

APPENDIX A: DETAILS OF CALCULATION OF DISTRIBUTION OF BLOCKAGE TIMES

We wish to solve the equation

$$\frac{\partial P}{\partial t'} = l_d \frac{\partial^2 P}{\partial x^2} - \frac{\partial P}{\partial x}, \quad (\text{A1})$$

where $t' = vt$, for $P(x, t')$ subject to the boundary conditions that P vanish at $x = 0, L$ and the initial condition $P(x, t' = 0) = \delta(x - x_0)$. The right and left eigenfunctions of $l_d \partial^2 / \partial x^2 - \partial / \partial x$ are respectively $\exp(x/2l_d) \sin(k_n x)$ and $\exp(-x/2l_d) \sin(k_n x)$, so we have

$$P(x, t') = \frac{2}{L} \sum_{n=1}^{\infty} e^{-\lambda_n t'} e^{-x_0/2l_d} \sin(k_n x_0) e^{x/2l_d} \sin(k_n x), \quad (\text{A2})$$

with $k_n = n\pi/L$ and $\lambda_n = l_d k_n^2 + 1/4l_d$. After taking a derivative with respect to x , setting $x = L$, and simplifying, one finds that the probability that the polymer will exit the channel at $x = L$ at time t' is

$$\varphi(t') = j(L) = -\frac{2l_d}{L} e^{(L-x_0)/2l_d} \times \sum_n e^{-\lambda_n t'} k_n \sin[k_n(x_0 - L)]. \quad (\text{A3})$$

Note that for large L this is a very slowly convergent series. It is thus convenient to rewrite it using the Poisson resummation formula. This formula states that for any function f , $\sum_{n=-\infty}^{\infty} f(n) = \sum_{m=-\infty}^{\infty} \hat{f}(2\pi m)$, where \hat{f} is the Fourier transform of f defined by $\hat{f}(q) = \int dx f(x) e^{iqx}$. Rewriting the sum in terms of the Fourier transform of the summand moves L from the denominator to the numerator of the exponential, yielding, after a little algebra,

$$\begin{aligned}
\varphi(t') &= \frac{1}{2\sqrt{\pi l_d t'^3}} e^{(L-x_0)/2l_d} e^{-t'/4l_d} \\
&\times \sum_{n=1,3,5,\dots} e^{-(n-1)L/2l_d} \\
&\times \left[(nL - x_0) e^{-(t'-nL+x_0)^2/4l_d t'} \right. \\
&\quad \left. - (nL + x_0) e^{-x_0/l_d} e^{-(t'-nL-x_0)^2/4l_d t'} \right]. \quad (\text{A4})
\end{aligned}$$

With φ written in this form, the first term is exponentially larger than all subsequent terms as L becomes large, facilitating the analysis of limiting cases. With the help of a few definite integrals a number of results can be obtained exactly. In particular, if one defines $I(\alpha) = \int_0^\infty dy/y^\alpha \exp[-(y-1)^2/4\gamma y]$, then $I(3/2) = I(1/2) = 2\sqrt{\pi\gamma}$. The first equality can be proven with the substitution $z = 1/y$, the second with the substitution $u = (y-1)/\sqrt{\gamma}$; $I(\alpha)$ for other values of α may be obtained by successive integrations by parts. Using these identities, one can show, for example, that the total probability that the polymer will exit from the *trans* side ($x = L$) if it started at x_0 is

$$\begin{aligned}
\int_0^\infty dt' \varphi(t') &= \left(1 - e^{-x_0/l_d}\right) \sum_{n=1,3,5,\dots} e^{-(n-1)L/2l_d} \\
&= \frac{1 - e^{-x_0/l_d}}{1 - e^{-L/l_d}}. \quad (\text{A5})
\end{aligned}$$

One can similarly obtain exact expressions for $\langle t' \rangle$ and for higher moments.

Thus far, we have allowed the polymer's starting point x_0 to be arbitrary. Since the polymer always starts entirely on the *cis* side of the channel, the case of interest to us is $x_0 \rightarrow 0$. Eq. (A5) shows that the probability that the polymer passes through the pore vanishes in this limit. This conclusion is, however, a pathology of our model. We can still obtain a meaningful *conditional* distribution of passage times (that is, a distribution of passage times for those polymers that do leave at $x = L$) by normalizing φ by the total probability of passage. In the limit $x_0 \rightarrow 0$, one obtains

$$\begin{aligned}
\psi(t') &= \lim_{x_0 \rightarrow 0} \left[\frac{1 - e^{-L/l_d}}{1 - e^{-x_0/l_d}} \varphi(t') \right] \\
&= 2\sqrt{\frac{l_d}{\pi t'^3}} \left(1 - e^{-\frac{t'}{l_d}}\right) \\
&\times \sum_{n=1,3,5,\dots} \left(\frac{n^2 L^2}{l_d t'} - 2 \right) e^{-\frac{(n-1)L}{2l_d}} e^{-\frac{(t'-nL)^2}{4l_d t'}}. \quad (\text{A6})
\end{aligned}$$

All the terms but the first are subdominant as $L \rightarrow \infty$, and when they are dropped, we obtain (4). Note that not only is Eq. 4 the correct asymptotic form for large L , but also that all subsequent terms describe peaks centered at increasingly larger values of t' . Thus, even when these terms significantly modify the behavior of $\psi(t')$ as $t' \rightarrow \infty$, they can have a very small effect in the vicinity of t_{\max} .

APPENDIX B: DETAILS OF CALCULATION OF MOBILITY AND DIFFUSION COEFFICIENT

Exact Expressions

In this appendix, we will derive the expression of Eq. 9 for the mean drift velocity v of a particle in a periodic potential and an analogous expression for the effective diffusion coefficient D . Since the linear operator \mathcal{L} (defined by Eq. 8) is periodic, it must have eigenfunctions of the Bloch form $\psi_n^R(k, x) = e^{ikx} u_n^R(k, x)$, where $|k| < \pi/a$ and $u_n^R(k, x)$ is periodic with period a . The eigenfunction $\psi_n^R(k, x)$ is defined by $\mathcal{L}\psi_n^R(k, x) = -\lambda_n(k)\psi_n^R(k, x)$. Since \mathcal{L} is a non-hermitian operator, right and left eigenfunctions are not equal, so we distinguish between them with superscripts R and L. Likewise, the eigenvalues $\lambda_n(k)$ are not in general real. The eigenfunctions are labelled by a band index n and a wavevector k in the first Brillouin zone. If the polymer starts at $x = x_0$ at $t = 0$, then $P(x, t)$ may be expressed as an eigenfunction expansion:

$$P(x, t) = \sum_n \int_{\text{BZ}} dk e^{ik(x-x_0)} u_n^L(k, x_0)^* u_n^R(k, x) e^{-\lambda_n(k)t}. \quad (\text{B1})$$

Because of the exponential decay $e^{-\lambda_n(k)t}$, the smallest values of $\text{Re } \lambda_n(k)$ determine the behavior of P at long times. One can prove that the lowest value occurs at $\lambda_0(k=0) = 0$. Performing a saddle point integration about this point, one thus finds that as $t \rightarrow \infty$,^{††}

$$P(x, t) \simeq \frac{1}{\sqrt{4\pi Dt}} e^{-(x-x_0-vt)^2/(4Dt)} u_0^R(k=0, x), \quad (\text{B2})$$

where

$$v = -i \left. \frac{d\lambda_0}{dk} \right|_{k=0} \quad \text{and} \quad D = 2 \left. \frac{d^2 \lambda_0}{dk^2} \right|_{k=0}. \quad (\text{B3})$$

At long times $P(x, t)$ is thus a spreading Gaussian, modulated by a periodic function $u_0^R(k=0, x)$ that gives detailed structure on the scale of a . One can hence reasonably interpret the constants v and D in the expression for the Gaussian envelope as the same constants that appear in the macroscopic Eq. 3.

In light of these expressions, we obviously want to study the behavior of λ_0 in the vicinity of $k = 0$. To do this, it is convenient to rephrase the eigenvalue condition $\mathcal{L}\psi_n^R(k, x) = \lambda_n(k)\psi_n^R(k, x)$ in terms of $u_n^R(k, x)$ as

^{††}Note that this result is valid only for values of x such that the difference $x - x_0 - vt \ll \mathcal{O}(\sqrt{t})$ for large t , so that the quantity in the exponential has a saddle point exactly at $k = 0$ instead of somewhere in the upper complex k half-plane.

$$\begin{aligned}
D_0 \left(\frac{\partial}{\partial x} + ik \right) & \left[\left(\frac{\partial}{\partial x} + ik \right) + \frac{\Phi'(x)}{k_B T} \right] u_n^R(k, x) \\
& = D_0 \left[\mathcal{L} + ik \left(2 \frac{\partial}{\partial x} + \frac{\Phi'(x)}{k_B T} \right) - k^2 \right] u_n^R(k, x) \\
& = -\lambda_n(k) u_n^R(k, x). \tag{B4}
\end{aligned}$$

If we view the k -dependent part of the operator on the left as a small perturbation on \mathcal{L} , then finding the derivatives of $\lambda_0(k)$ at $k = 0$ is formally the same as a problem in quantum-mechanical perturbation theory.^{‡‡} As usual, we pose the expansions

$$\begin{aligned}
\lambda_0(k) & = k \left. \frac{d\lambda_0}{dk} \right|_{k=0} + \frac{k^2}{2} \left. \frac{d^2\lambda_0}{dk^2} \right|_{k=0} + \dots \\
u_0^R(k, x) & = u_0^R(0, x) + k u_0^{R,1}(x) + \dots \\
u_0^L(k, x) & = u_0^L(0, x) + k u_0^{L,1}(x) + \dots. \tag{B5}
\end{aligned}$$

The “ground state” $u_0^R(k = 0, x)$ of the unperturbed problem can be obtained exactly by integrating $\mathcal{L}u_0^R(k = 0, x) = 0$ (Riskin, 1984):

$$u_0^R(k = 0, x) = N e^{-\Phi(x)/k_B T} - \frac{S}{D_0} \int_0^x dx' e^{\Phi(x')/k_B T}. \tag{B6}$$

The two constants of integration N and S are determined by normalization and by requiring that $u_0^R(k = 0, x)$ be periodic. Physically, S is the (constant) probability current density in the stationary state $u_0^R(k = 0, x)$. Since $\mathcal{L}^\dagger = D_0 \left[\frac{\partial}{\partial x} - \frac{\Phi'}{k_B T} \right] \frac{\partial}{\partial x}$, $u_0^L(k = 0, x)$ is clearly a constant, which we choose to be 1. The first correction to $\lambda_0(k = 0)$ is then just the “expectation value” of the perturbation in the “ground state”:

$$\left. \frac{d\lambda}{dk} \right|_{k=0} = iv = i \int_0^a dx \left(2 \frac{\partial}{\partial x} + \frac{\Phi'(x)}{k_B T} \right) u_0^R(k = 0, x). \tag{B7}$$

After a bit of algebra, one obtains

$$v = Sa = D_0 a \frac{(1 - e^{-Fa/k_B T})}{a^2 [I_1 I_2 - (1 - e^{-Fa/k_B T}) I_3]}, \tag{B8}$$

where

$$I_1 = \int_0^a \frac{dx}{a} e^{\Phi(x)/k_B T}, \tag{B9}$$

$$I_2 = \int_0^a \frac{dx}{a} e^{-\Phi(x)/k_B T}, \text{ and} \tag{B10}$$

$$I_3 = \int_0^a \frac{dx}{a} \int_0^x \frac{dx'}{a} e^{-\Phi(x)/k_B T} e^{\Phi(x')/k_B T}. \tag{B11}$$

^{‡‡}There is a slight difference in that in our case the perturbation to the original operator \mathcal{L} has terms of order k^2 as well as of order k .

Note that the integrals $I_1^{(0)}$ and $I_2^{(0)}$ defined in Eq. 11 are just I_1 and I_2 evaluated with $F = 0$. Finally, v may be put in the form of Eq. 9 by everywhere rescaling a as $a \mapsto na$ and letting $n \rightarrow \infty$ (le Doussal and Vinokur, 1995; Scheidl, 1995). This substitution is valid because we could have originally thought of $U(x)$ as having period na instead of a for any positive integer n .

To find the $\mathcal{O}(k^2)$ correction to $\lambda_0(k = 0)$ requires knowing the $\mathcal{O}(k)$ correction to the ground state $u_0^{R,1}(x)$. This is typically expressed as a sum of eigenfunctions of the unperturbed problem, which are assumed known. Instead, we will invert \mathcal{L} by direct integration to find an analytic expression for $u_0^{R,1}(x)$. After substituting the expansions of Eq. B5 into the eigenvalue equation and equating terms of order k , we find

$$\begin{aligned}
\mathcal{L}u_0^{R,1}(x) & = -iv u_0^R(k = 0, x) \\
-iD_0 \left(2 \frac{\partial}{\partial x} + \frac{\Phi'(x)}{k_B T} \right) u_0^R(k = 0, x). \tag{B12}
\end{aligned}$$

Everything on the right hand side of the equation is known, so $u_0^{R,1}(x)$ can be found by integrating twice. The constants of integration are determined by demanding that $u_0^{R,1}(x)$ be periodic and that its inner product with $u_0^L(k = 0, x) = 1$ vanish. Once $u_0^{R,1}(x)$ is known, we can equate terms of order k^2 to learn that

$$D - D_0 = \int_0^a u_0^L(k = 0, x)^* i \left(2 \frac{\partial}{\partial x} + \frac{\Phi'(x)}{k_B T} \right) u_0^{R,1}(x). \tag{B13}$$

A certain amount of additional algebra finally leads to an expression for D :

$$\frac{D}{D_0} = 1 + L \frac{I_2 J_1 - (1 - e^{-Fa/k_B T}) J_2}{I_1 I_2 - (1 - e^{-Fa/k_B T}) I_3} - J_3, \tag{B14}$$

where the I_i are the same as before,

$$J_1 = \int_0^a \frac{dx}{a} \int_0^x \frac{dx'}{a} e^{\Phi(x)/k_B T} f(x'), \tag{B15}$$

$$J_2 = \int_0^a \frac{dx}{a} \int_0^x \frac{dx'}{a} \int_0^{x'} \frac{dx''}{a} e^{-\Phi(x)/k_B T} e^{\Phi(x')/k_B T} f(x''), \tag{B16}$$

$$J_3 = \int_0^a \frac{dx}{a} \int_0^x \frac{dx'}{a} f(x'), \tag{B17}$$

and

$$f(x) = \frac{Sa}{D_0} u_0^R(k = 0, x) + \frac{\partial u_0^R(k = 0, x)}{\partial x} - \frac{S}{D_0}. \tag{B18}$$

Just as with the expression of Eq. B8 for the velocity, we can find equivalent formulas for D by replacing a by na and letting $n \rightarrow \infty$.

Approximate Expressions

Having obtained exact expressions for v and D , we will now outline how the limiting forms of Eq. 10 through Eq. 14 are derived. We will focus on the expressions for v ; the manipulations required to obtain the analogous asymptotic forms for D are very similar.

The behavior of v for large and small F is most easily studied starting from Eq. 9. Define $A(z) \equiv \int_0^a dx/a \exp[U(x+z)/k_B T - U(x)/k_B T]$, and note that A is a periodic function of z with period a . Expanding $A(z)$ in a Fourier series and Laplace transforming term by term as demanded by Eq. 9 leads immediately to the formula of Eq. 10 for the small F behavior; in particular, the leading behavior is determined by the constant term in the series, $\int_0^a dz/a A(z) = I_1^{(0)} I_2^{(0)}$. Similarly, we may find the behavior of v for large F by successive integrations by parts: $D_0/v = A(0)/F + A'(0)/F^2 + \dots$.

The starting point for finding the large U behavior is similar. Rewrite v as

$$\frac{D_0 a}{v} = \int_0^a dx e^{-U(x)/k_B T} e^{Fx/k_B T} \times \int_x^\infty dy e^{U(y)/k_B T} e^{-Fy/k_B T}. \quad (\text{B19})$$

First the inner, and then the outer integral can then be evaluated by Laplace's method as U becomes large. Note that since $U(x)$ is periodic, we must sum a geometric series over an infinite number of extrema to find the asymptotic expression for the inner integral. Also, the location of the first maximum depends on the lower bound of integration x . Once the two integrals have been evaluated, an expression equivalent to Eq. 14 follows immediately. The only difference is that in Eq. 14, we have chosen to write $I_1^{(0)}$ and $I_2^{(0)}$ instead of their large U forms.

APPENDIX C: ESTIMATE OF REDUCTION IN THE DRIVING FORCE

In the discussion section, we mentioned two factors that should reduce the driving force F on the polymer from the naive value $Fa/k_B T \approx 5$. In this appendix, we present order-of-magnitude estimates of how large a correction these effects cause. The estimates are based on the equations of continuum mechanics in a simplified geometry and use bulk parameter values. They thus neglect a number of subtleties, most notably the presence of significant numbers of charged groups on the α -hemolysin pore itself.

We begin by looking at the additional drag on the polyelectrolyte due to the flow of oppositely charged small ions through the pore. Consider a cylindrical polymer of radius r inside a cylindrical pore of radius R , and assume that the distance $\delta = R - r$ between the polymer and the pore satisfies $\delta \lesssim r$ and $\delta \lesssim \kappa^{-1}$, where κ^{-1} is

the Debye-Hückel screening length. Both conditions hold in KBBD's experiments. Then neither the steady-state density n of ions nor the solvent velocity u parallel to the cylinder axis vary too strongly with radial distance. In particular, there is no Manning condensation. In the presence of an applied electric field \mathbf{E} (of order the applied voltage V divided by the length of the channel), a body force term $en\mathbf{E}$ must be added to the Stokes equation that describes very viscous flow. Here e is the electron charge, and we have assumed that the only ions present are monovalent cations; the figure we obtain for the additional drag will thus be an upper bound on the drag possible with ions of both signs. We may use the component of the Stokes equation along the cylinder axis to estimate

$$enE \sim \eta \frac{u_i}{\delta^2}, \quad (\text{C1})$$

where η is the solvent viscosity. Since the Stokes equation is linear, we have written the axial solvent velocity as $u = u_p + u_i$, where u_i is driven by the electrical force on the ions, and u_p by the motion of the polymer. The electrical current density J due to the ions is then roughly

$$J \sim e^2 n \mu E + en(u_p + u_i). \quad (\text{C2})$$

Here μ is the mobility of a single counterion. The first term describes motion of the counterions relative to the solvent, and the second the convection of the counterions by solvent motion. The value of J is set by the fact that the total current $I \sim 2\pi r \delta J$ is known to be of order 10 pA in KBBD's experiments; u_p must be of order the polymer's translocation speed. Thus, the problem is reduced to solving the two "equations" C1 and C2 in the two unknowns n and u_p . By substituting reasonable parameter values, one finds that the term proportional to $u_p + u_i$ in Eq. C2 may be dropped. Then, the extra drag force per length on the polymer is

$$\frac{\text{drag}}{\text{length}} \sim 2\pi r \frac{\eta u_i}{\delta} \sim \frac{I}{\mu e} \quad (\text{C3})$$

Substituting a typical value of an ionic mobility (in bulk solution), and multiplying by the channel's length $l_{\text{ch}} \sim 50\text{\AA}$, we obtain a drag force of order 10^{-7} dyne due to the ion-driven solvent flow. This is to be compared to $5k_B T/a \approx 3 \times 10^{-6}$ dyne. We conclude that the presence of the counterions in the channel does not significantly reduce F .

Another factor that we should take into account concerns the assumption that any applied voltage drop V falls entirely across the channel. In reality, some electric field must "leak" out of the pore, decreasing the force that drives the polymer. The simplest model in which one can consider this problem assumes that the bulk solution is neutral and has a constant conductivity σ , so that the electrical current density and the electric field are related by $\mathbf{J} = \sigma \mathbf{E}$. This picture of course does not hold within a distance κ^{-1} of the membrane, but should

be reasonably accurate on longer length scales. Focus only on one side of the membrane, so that the pore acts as a current source injecting a current I at the boundary of an infinite half-space. Far away from the pore, the current density, and thus the electric field, should decay like $1/r^2$. In the near field, one expects this decay to be cut off at a distance of order the pore radius R . Knowing the current I , we can immediately obtain the electric potential, and thus the voltage drop V_c across the channel, in terms of the voltage V imposed at infinity. Our rough estimate gives (in cgs units)

$$V - V_c \sim 2 \int_{\infty}^R \frac{I}{2\pi\sigma r^2} dr \sim \frac{I}{\pi\sigma R}. \quad (\text{C4})$$

The factor of 2 in front of the integral arises because we must include the effect of a voltage decrease on both sides of the membrane. Substituting experimental values for I , σ , and R , we find that this calculation suggests that V_c differs from V by only a few percent.

It is a pleasure to thank Dan Branton and Jene Golovchenko for introducing us to this problem and for numerous helpful discussions. We would also like to thank Armand Ajdari, Meredith Betterton, Jean-François Joanny, Didier Long, and Sergei Obukhov for insightful comments and for pointing out useful references. This work was supported by the Harvard Materials Research Science and Engineering Laboratory through Grant No. DMR94-00396 and by the National Science Foundation through Grant No. DMR97-14725. One of us (D.K.L.) also acknowledges support from a National Science Foundation Graduate Research Fellowship.

Achter, E. K. and G. Felsenfeld. 1971. The conformation of single-strand polynucleotides in solution: Sedimentation studies of apurinic acid. *Biopolymers* 10: 1625-1634.

Ambegokar, V. and B. I. Halperin. 1969. Voltage due to Thermal Noise in the DC Josephson Effect. *Phys. Rev. Lett.* 22: 1364-1366.

Attardi, G. and G. Schatz. 1988. Biogenesis of mitochondria. *Annu. Rev. Cell Biol.* 4:289-333.

Bezrukov, S. M., I. Vodyanoy, R. A. Brutyan, and J. J. Kasianowicz. 1996. Dynamics and free energy of polymers partitioning into a nanoscale pore. *Macromolecules* 29:8517-8522.

Binder, K. 1983. Critical behavior at surfaces. In C. Domb and J. L. Lebowitz eds., *Phase Transitions and Critical Phenomena*, vol 8. Academic: London.

Bouchaud, J. P. and A. Georges. 1990. Anomalous diffusion in disordered media: Statistical mechanisms, models, and physical applications. *Phys. Rep.* 195: 127-293.

Burlatsky, S. F. and J. M. Deutch. 1993. Influence of solid friction on polymer relaxation in gel electrophoresis. *Science*. 260: 1782-1784.

Burlatsky, S. F. and J. M. Deutch. 1995. Solid friction in gel electrophoresis. *J. Chem. Phys.* 103: 8216-8227.

Cantor, C. R. and P. R. Schimmel. 1980. *Biophysical Chemistry*. Freeman: San Francisco.

Carl, W. 1998. A polymer threading a membrane: Model system for a molecular pump. *J. Chem. Phys.* 108: 7921-7922.

Citovsky, V. and P. Zambryski. 1993. Transport of nucleic acids through membrane channels: Snaking through small holes. *Annu. Rev. Microbiol.* 47: 167-197.

de Gennes, P. G. 1979. *Scaling Concepts in Polymer Physics*. Cornell UP: Ithaca.

Deutsch, J. M. 1987. Dynamics of pulsed-field electrophoresis. *Phys. Rev. Lett.* 59: 1255-1258.

Deutsch, J. M. and Hyoungsoo Yoon. 1997. Macromolecular separation through a porous surface. *J. Chem. Phys.* 106: 9376-9381.

Di Marzio, E. A. and A. J. Mandell. 1997. Phase transition behavior of a linear macromolecule threading a membrane. *J. Chem. Phys.* 107: 5510-5514.

Doi, M. and S. F. Edwards. 1986. *The Theory of Polymer Dynamics*. Clarendon: Oxford.

Dreiseikermann, B. 1994. Translocation of DNA across bacterial membranes. *Microbiol. Rev.* 58: 293-316.

Fisher, D. S., P. le Doussal, and C. Monthus. 1998. Random walks, reaction-diffusion, and nonequilibrium dynamics of spin chains in one-dimensional random environments. *Phys. Rev. Lett.* 80: 3539-3542.

Haken, H., H. Sauermann, Ch. Schmid, and H. D. Vollmer. 1967. Theory of Laser Noise in the Phase Locking Region. *Z. für Phys.* 206: 369-393.

Hanss, B., E. Leal-Pinto, L. A. Bruggeman, T. D. Copeland, and P. E. Klotman. 1998. Identification and characterization of a cell membrane nucleic acid channel. *Proc. Natl. Acad. Sci. USA* 95: 1921-1926.

Herzel, H., E. N. Trifonov, O. Weiss, and I. Große. 1998. Interpreting correlations in biosequences. *Physica A* 249: 449-459.

Jülicher, F., A. Ajdari, and J. Prost. 1997. Modeling molecular motors. *Rev. Mod. Phys.* 69: 1269-1281.

Jülicher, F. and R. Bruinsma. 1998. Motion of RNA polymerase along DNA: A stochastic model. *Biophys. J.* 74: 1169-1185.

Kasianowicz, John J. and Sergey M. Bezrukov. 1995. Protonation dynamics of the α -Toxin ion channel from spectral analysis of pH-dependent current fluctuations. *Biophys. J.* 69: 94-105.

Kasianowicz, John J., Eric Brandin, Daniel Branton, and David W. Deamer. 1996. Characterization of individual polynucleotide molecules using a membrane channel. *Proc. Natl. Acad. Sci. (USA)* 93: 13770-13773.

le Doussal, P. and Vinokur, V. 1995. Creep in one dimension and phenomenological theory of glass dynamics. *Physica C* 254: 63-68.

Lee, Namkyoung and Sergei Obukhov. 1996. Diffusion of a polymer chain through a thin membrane. *J. Phys II France* 6:195-204.

Park, P. J. and W. Sung. 1998a. Polymer release out of a

spherical vesical through a pore. *Phys. Rev. E* 57: 730–734.

Park, P. J. and W. Sung. 1998b. Polymer translocation induced by adsorption. *J. Chem. Phys.* 108: 3013–3018.

C.-K. Peng, S. V. Buldyrev, A. L. Goldberger, S. Havlin, F. Sciortino, M. Simons, and H. E. Stanley. 1992. Long-range correlations in nucleotide sequences. *Nature* 356: 168–170.

Peskin, Charles S., Garrett M. Odell, and George F. Oster, 1993. Cellular Motions and Thermal Fluctuations: The Brownian Ratchet. *Biophys. J.* 65:316–324.

Risken, H. 1984. The Fokker-Planck Equation. Springer-Verlag, Berlin.

Schatz, G. and B. Dobberstein. 1996. Common principles of protein translocation across membranes. *Science* 271:1519–1526.

Scheidl, S. 1995. Mobility in a one-dimensional disorder potential. *Z. Phys. B* 97: 345–352.

Simon, S.M. and G. Blobel. 1991. A protein-conducting channel in the endoplasmic reticulum. *Cell* 69: 677–684.

Simon, S. M., C. S. Peskin, and G. F. Oster. 1992. What drives the translocation of proteins? *Proc. Natl. Acad. Sci. (USA)* 89: 3770–3775.

Smith, S. B., Y. Cui, and C. Bustamante. 1996. Overstretching DNA: The elastic response of individual double-stranded and single-stranded DNA molecules. *Science* 271: 795–799.

Song, L., M. R. Hobaugh, C. Shustak, S. Cheley, H. Bayley, and J. E. Gouaux. 1996. Structure of staphylococcal α -hemolysin, a heptameric transmembrane pore. *Science* 274: 1859–1866.

Sung, W. and P. J. Park. 1996. Polymer translocation through a pore in a membrane. *Phys. Rev. Lett.* 77: 783–786.

Szabò, I., G. B athori, F. Tombola, M. Brini, A. Coppola, and M. Zoratti. 1997. DNA translocation across planar bilayers containing *Bacillus subtilis* ion channels. *J. Biol. Chem.* 272: 25275–25282.

Szab , I., G. B athori, F. Tombola, A. Coppola, I. Schmehl, M. Brini, A. Ghazi, V. De Pinto, and M. Zoratti. 1998. Double-stranded DNA can be translocated across a planar membrane containing purified mitochondrial porin. *FASEB J.* 12:495–502.

Tinland, B., A. Pluen, J. Sturm, and G. Weill. 1997. Persistence length of single-stranded DNA. *Macromolecules* 30: 5763–6765.

van Kampen, N. G. 1992. Stochastic Processes in Physics and Chemistry (2nd ed.). North-Holland, Amsterdam.

J.-L. Viovy and T. Duke. 1994. Technical comment. *Science*. 264: 112–113.

Yoon, Hyoungsoo and J. M. Deutsch. 1995. Dynamics of a polymer in the presence of permeable membranes. *J. Chem. Phys.* 102: 9090–9095.

FIG. 1. Histogram of number of observed blockade events versus the lifetime of the blockade, for 210 nucleotide poly[U]. The numbers 1 through 3 label the different peaks. From KBBB (courtesy of Dan Branton, Harvard University). *Inset*: Typical time series of the current versus time in the experiments of KBBB, showing a transient blockade due to the translocation of a polymer (courtesy of Dan Branton, Harvard University).

FIG. 2. The distribution $\psi(t)$ of passage times plotted versus t for $L/l_d = 5$. Both quantities are appropriately non-dimensionalized, t as vt/L and $\psi(t)$ as $L\psi(t)/v$. The dashed curve is a Gaussian with the same mean and variance as $\psi(t)$.

FIG. 3. Plot of the relative width $\delta t/t_{\max}$ of the peak in the distribution of passage times, versus l_d/L . This curve may be used to obtain the quick estimate $l_d \approx 40$ nucleotides for the system studied by KBBB. The dashed curve gives the $L \rightarrow \infty$ asymptotic behavior, $\delta t/t_{\max} \sim \sqrt{2l_d/L}$. We have chosen to put l_d/L instead of L/l_d along the ordinate to allow smooth contact with this large L behavior.

FIG. 4. vt_{\max}/L plotted versus L/l_d . Note that vt_{\max}/L varies significantly over the range of L/l_d relevant to the experiments of KBBB, and in particular that it does not reach its asymptotic value of unity until well outside the range of this plot. *Inset*: Plot of t_{\max} (nondimensionalized by l_d/v) versus L (nondimensionalized by l_d). The dashed line gives the large L limiting form L/v , the solid line the exact value. Note that although t_{\max} appears to the eye to depend linearly on L over much of the range of the plot, it still differs significantly from L/v .

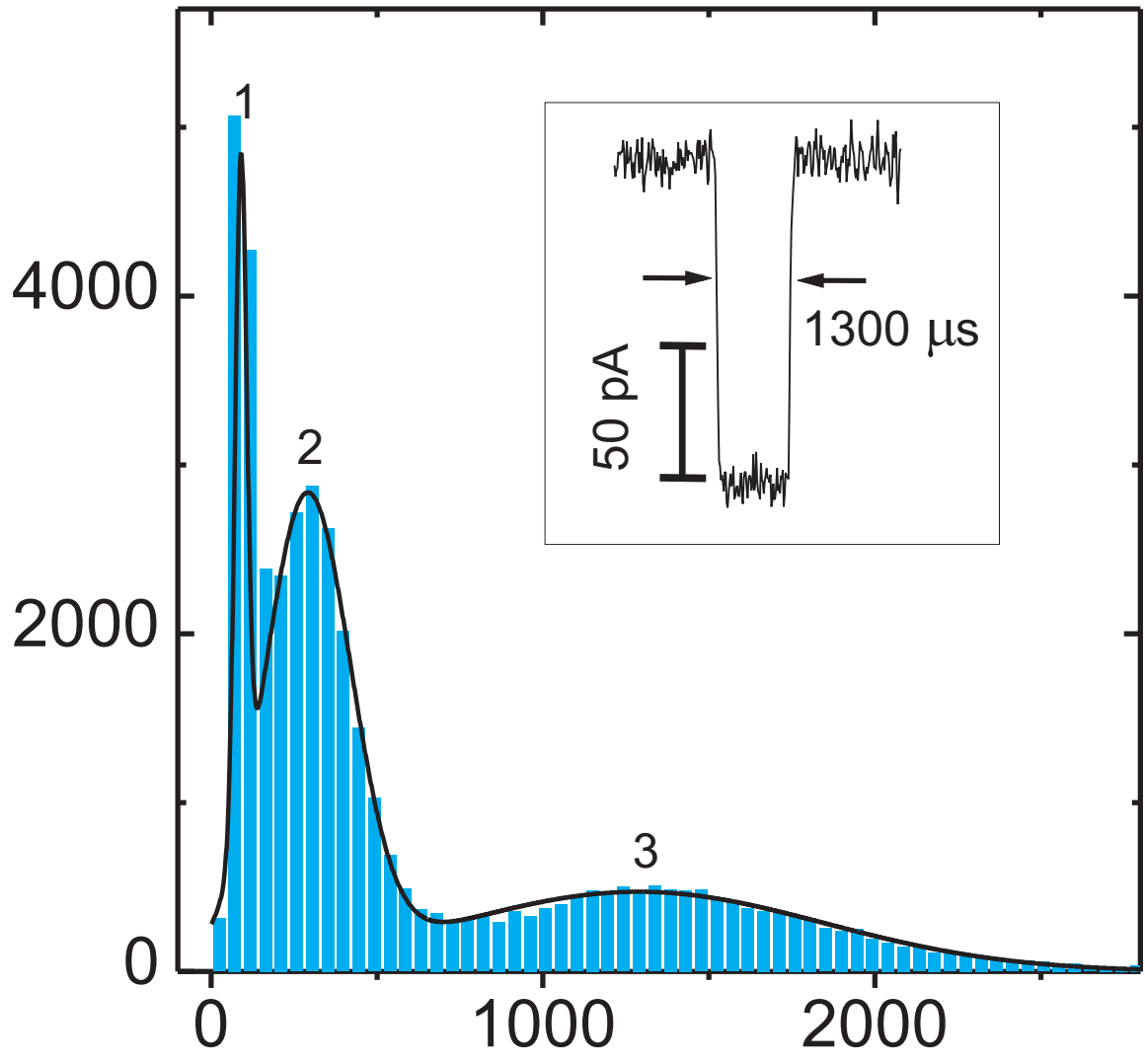
FIG. 5. Sketch of the sawtooth “cartoon” potential discussed in the text. The potential has period a , and αa is the distance from one minimum to the next maximum. The parameter U_0 gives the energy difference between minimum and maximum.

FIG. 6. Sketch showing how asymmetry in the potential can lead to different speeds for forwards and backwards motion. A bias is applied to the unperturbed potential (A) at top so that it has the same average gradient in the two bottom pictures. The potential at right (B), however, has been reflected through the vertical axis before the gradient is applied. It thus has larger barriers to hopping from one minimum to the next than the potential at left (C), leading to slower dynamics.

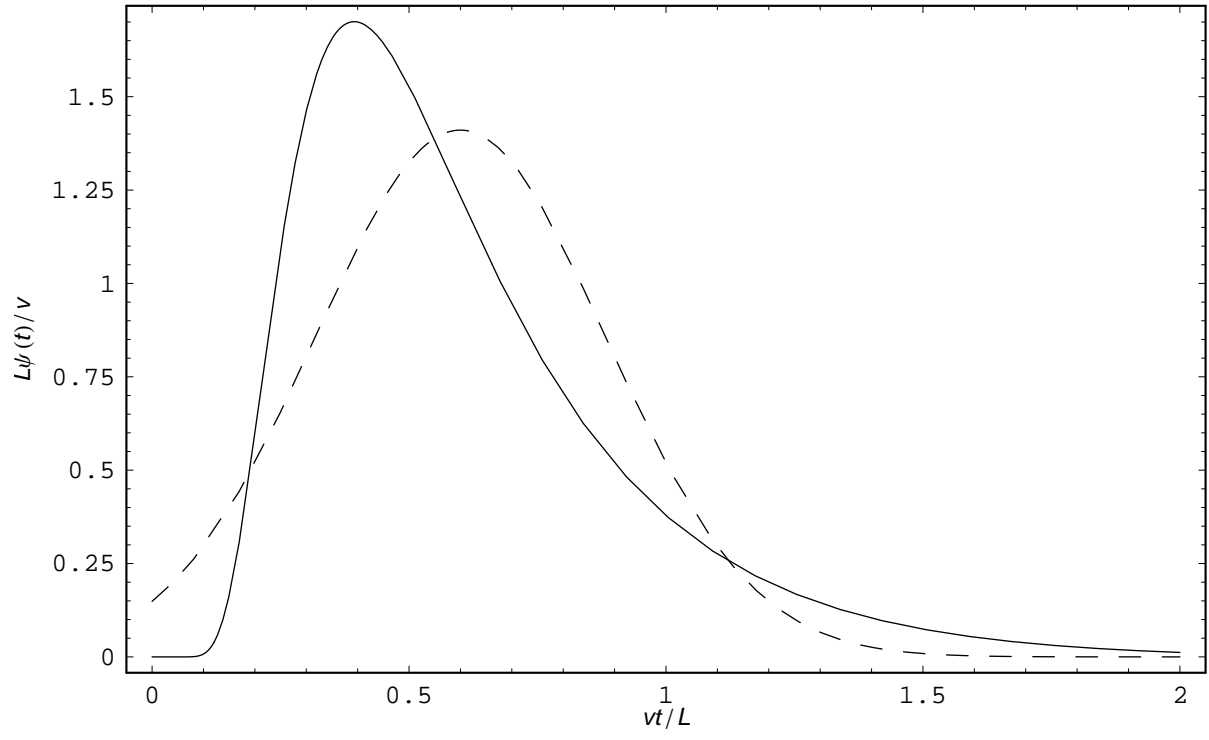
FIG. 7. The four possible relative orientations of polymer, pore, and applied electric field. In KBBB's experiments, the relative orientation of the pore and field is fixed and the orientation of the polymer is allowed to vary, corresponding to cases B and D. In our microscopic model, the pairs (A, B) and (C, D) are related by $F \mapsto -F$.

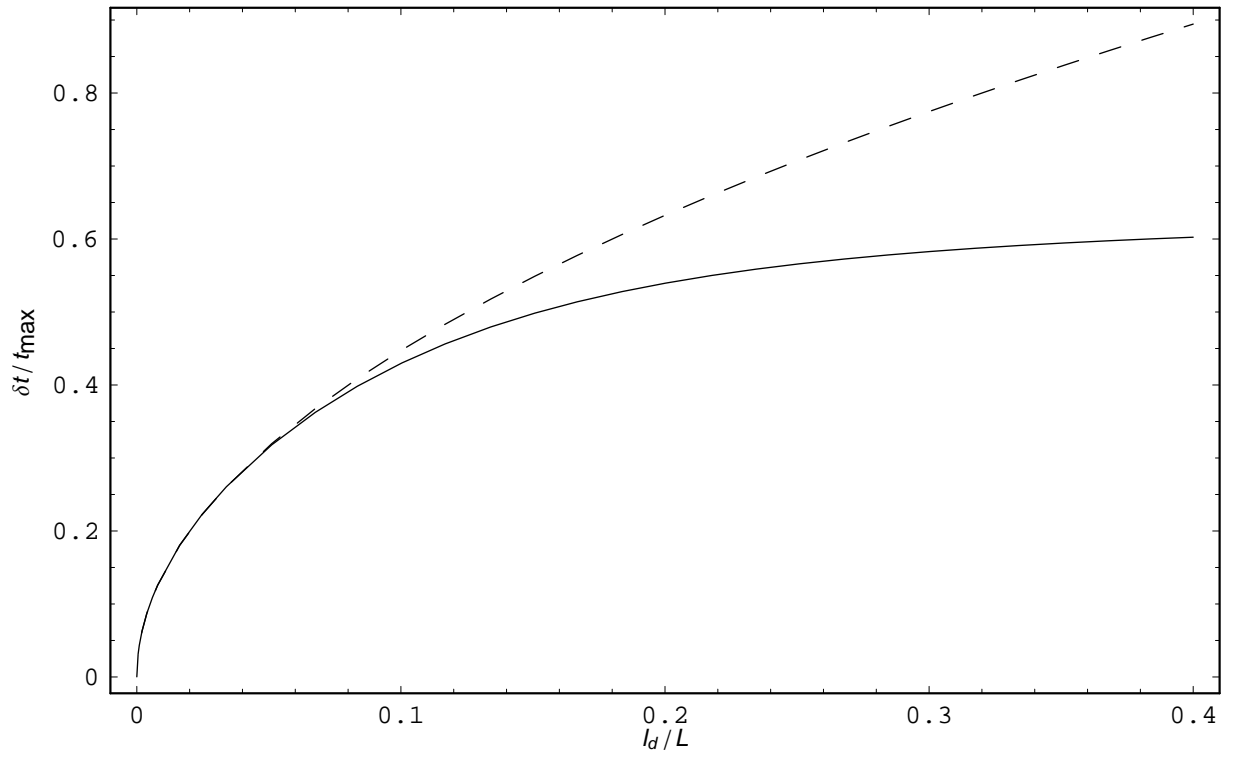
FIG. 8. Plot of the (nondimensionalized) average velocity v from equation 9 versus the driving force $Fa/k_B T$; v is calculated using our microscopic model with a sawtooth potential. The parameter values are $U_0/k_B T = 10$; $\alpha = 0.7$ for the upper curve and $\alpha = 0.3$ for the lower curve. The potentials for the two curves are thus related by $U(x) \mapsto U(-x)$. *Inset*: The diffusive length l_d versus the barrier height U_0 of the sawtooth potential, for fixed driving force $Fa = 5k_B T$ and asymmetry $\alpha = 0.7$. Note that over the entire range of U_0 , $l_d \lesssim a$.

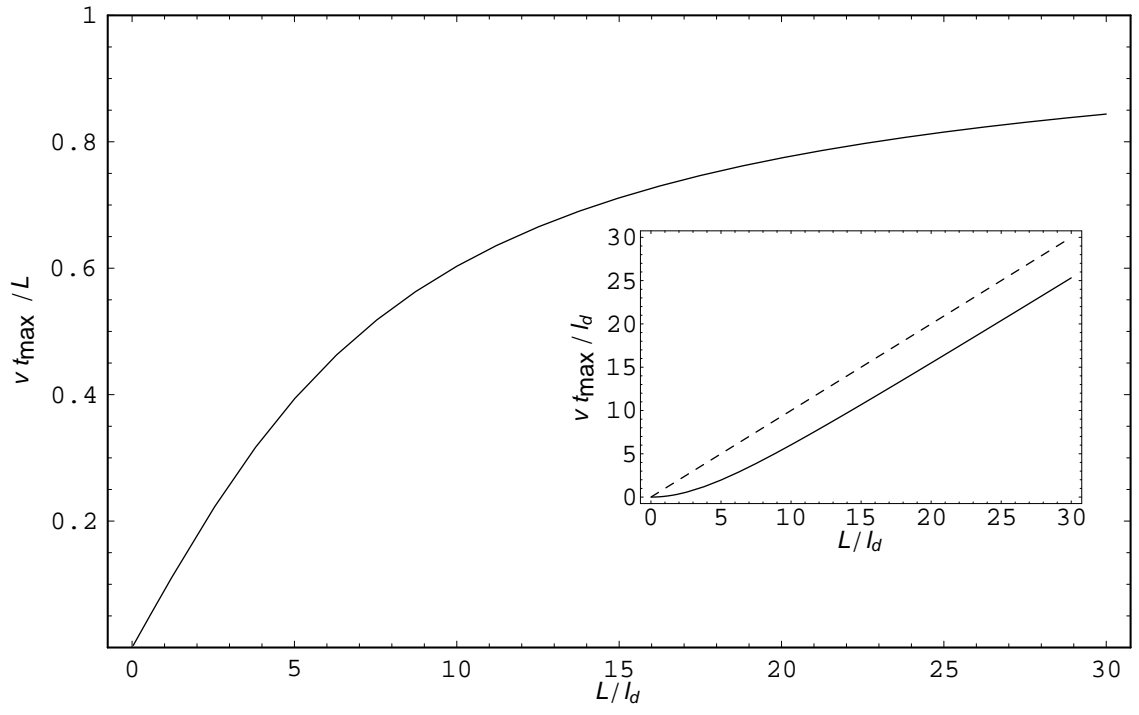
Number of Blockades

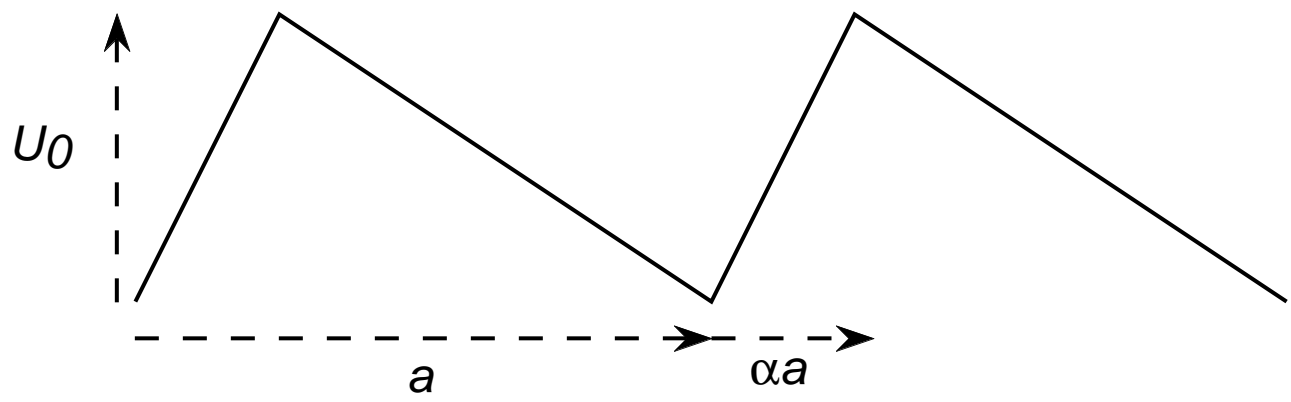


Lifetime (μs)









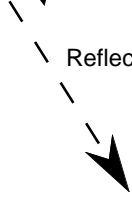
A.



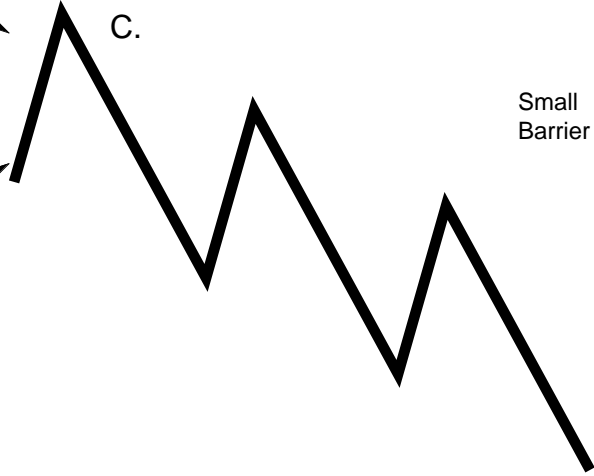
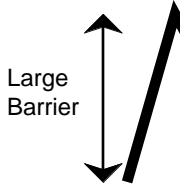
Tilt



Reflect then tilt



C.



B.

